OSCA, an Optimised Stellar Coronagraph for Adaptive optics: Description and first light

Samantha Thompson [a*], Peter Doel [a*], Richard Bingham [a], Andrew Charalambous [a], Nirmal Bissonauth [b], Paul Clark [b], Richard Myers [b], Gordon Talbot [c]

[a] University College London, Department of Physics and Astronomy, Gower Street, London, UK
[b] University of Durham, Astronomical Instrumentation Group, South Road, Durham, UK
[c] Isaac Newton Group of Telescopes, Santa Cruz de la Palma, Tenerife, Spain

ABSTRACT

We describe a coronagraph facility built for use with the 4.2 metre William Herschel Telescope (WHT) and its adaptive optics system (NAOMI). The use of the NAOMI adaptive optics system gives an improved image resolution of ~0.15 arcsec at a wavelength of 2.2 microns. This enables our Optimised Stellar Coronagraph for Adaptive optics (OSCA) to null stellar light with smaller occulting masks and thus allows regions closer to bright astronomical objects to be imaged. OSCA is a fully deployable instrument and when in use leaves the focus of the NAOMI beam unchanged. This enables OSCA to be used in conjunction with a number of instruments already commissioned at the WHT. The main imaging camera to be used with OSCA will be INGRID; a 1024x1024 HgCdTe cooled SWIR detector at the NAOMI focus. OSCA can also be used in conjunction with an integral field spectrograph for imaging at visible wavelengths. OSCA provides a selection of 10 different occulting mask sizes from 0.25 – 2.0 arcsec and some with a novel gaussian profile. There is also a choice of 2 different Lyot stops (pupil plane masks). A dichroic placed before the AO system can give us improved nulling when occulting masks larger than the seeing disk are used. We also present results from initial testing and commissioning at the William Herschel Telescope.

Keywords: coronagraph, adaptive optics, astronomy

1. INTRODUCTION

As described in numerous other papers on the subject, adaptive optics teamed with a coronagraph provides an opportunity for several interesting science studies. Compared to a standard coronagraphic imaging system, one with adaptive optics gives much higher spatial resolution and a high dynamic range allowing the environments of bright objects to be studied closer in than ever before.[1, 2]

Adaptive optics (AO) is still a relatively expensive technology and so scientific return must be maximised to realise its full benefit. Science targets are also limited since most AO systems rely on bright stars for wavefront sensing. Thus an instrument suite for use with an AO system needs to be selected to maximise the science for the observable objects and optimised to match the capabilities of the AO system. Since August 2000 the WHT has been equipped with the NAOMI (Nasmyth Adaptive Optics for Multi-purpose Instrumentation) adaptive optics system.[3] The main correction element is a 76 segment mirror and gives almost diffraction limited wavefront correction at $\lambda = 2.2$ microns. At visible wavelengths NAOMI is able to perform partial wavefront correction. OSCA is a low cost addition to the suite of instrumentation that are fed by NAOMI and yet it has significantly increased the range of scientific observations that can be performed. Since NAOMI currently relies on bright natural guide stars and coronagraphy is used for observing the close vicinity of bright astronomical objects, then the two are an ideal coupling. In early 2003 an integral field spectrograph (OASIS) will also be added to the system for imaging at visible wavelengths. When used in conjunction with OSCA, OASIS could provide spectra of faint structure around bright sources. Since OSCA has an automatic and accurate deployment mechanism a whole range of interesting observation programs can be envisaged.

[*] Correspondence to SJT, email: sjt@star.ucl.ac.uk and APD, email: apd@star.ucl.ac.uk

2. DESCRIPTION

OSCA is a facility class instrument built for use at the Nasmyth focus of the WHT. It is a classic Lyot coronagraph[4] design, although two of the occulting masks have a gaussian profile instead of the standard hard edged disks of our other masks. OSCA has a selection of 10 focal plane masks (one for alignment purposes only), two pupil plane (Lyot) masks and is fully deployable. OSCA operates over the wavelength range 0.4 – 2.4 microns, although visible observations will only be possible after OASIS has been commissioned. The size restrictions, wavelength range and requirement for full automatic deployment made OSCA a design challenge in many respects. An important aim in the design of OSCA was to make it easy to deploy and use in order to save time whilst observing. As the OSCA occulting mask positions are all centred to within a few microns of each other, no re-alignment of the star is necessary between changes.

2.1 Optical design

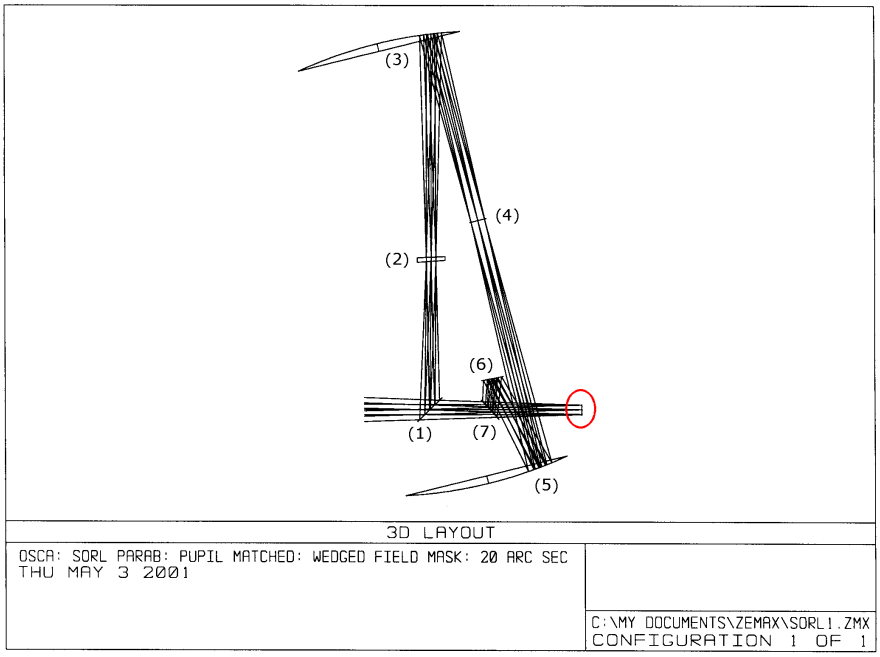

Figure 1. Optical design of OSCA. Original focal position without OSCA is shown circled.

The ultimate requirements in the optical design were to ensure that the NAOMI focal position was unaltered with OSCA deployed in the beam path (see Figure 1) and to fit this design into a very small spatial envelope. In order to accommodate the required wavelength range of 0.4 – 2.4 microns all mirrors in the system are coated with protected silver. In addition all transmissive optics are made from an I.R. grade fused silica (Spectrosil WF) which gives over 90% transmission across the entire specified wavelength range and can be polished to a very high surface accuracy.

The path of light through OSCA is shown in Figure 1 and is numbered sequentially along the beam direction. When deployed in the NAOMI beam, flat mirror (1) picks up the beam. The occulting masks are located at the focal plane (2). The Lyot stop is located at the pupil plane (4). The mirrors at (3) and (5) are a pair of off-axis paraboloids, and finally the flats at (6) and (7) position the focus to the original NAOMI focal position.

To prevent ghosting within OSCA the substrates for the focal plane masks have a wedge angle of 1.5°. The standard focal plane (occulting) masks are made of chromium and were created using photolithography techniques. We also had two full greyscale gaussian masks manufactured for us by Canyon Materials Ltd. Their patented glass works in much the same way as a photographic plate in that an electron beam is used to ‘expose’ the glass to achieve the required

greyscale levels. However, the transmission function of the glass means that it is only suitable for use in visible light (0.4 – 0.8 microns). The pupil plane masks are manufactured from 0.25mm thin, hard stainless steel by a process of photo-chemical machining. The field of view for OSCA is designed to be 20 arcsec but ghosting within the INGRID camera optics has currently reduced this to 15 arcsec.

2.2 Mechanical design

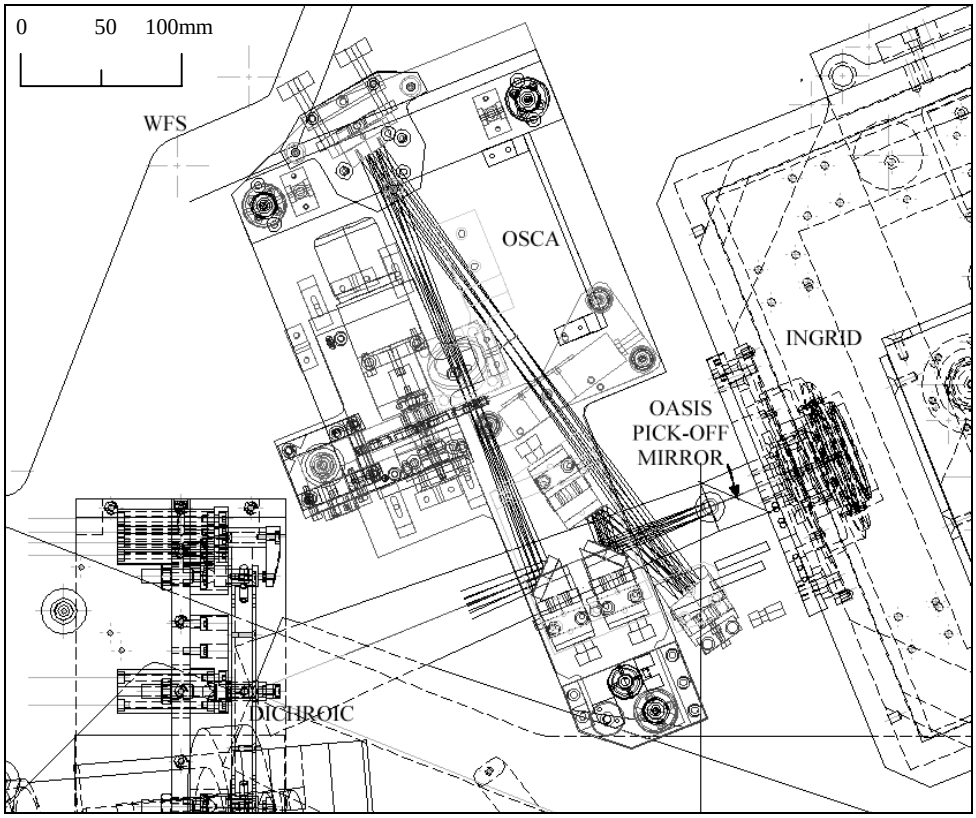

Figure 2. CAD diagram of OSCA with reference to surrounding instrumentation.

The design of OSCA meets its performance requirements by using kinematic referencing wherever possible, providing precise adjustment and repeatable positioning of the active parts of the system. Commercially available components are used where possible.

Structurally, OSCA consists of two horizontal plates with the opto-mechanics sitting on the top plate. The lower horizontal plate sits on the GHRIL table. It is positioned by screw adjusters and clamped rigidly to the table. The top plate is spaced from the lower plate by 3 vertical fine thread ball tipped screws with kinematic location, which provide height and tilt adjustment for the complete optical system.

The unit can be automatically deployed to interrupt the beam passing through to INGRID and the OASIS pick-off mirror. Space restrictions on the GHRIL table only allow vertical deployment, and by using the existing kinematic system this is a simple and reliable solution. Removing OSCA from the light path is achieved by lowering the top plate at the incoming beam end. The flat and ball-tip adjuster separate, allowing the top plate to rotate about the groove and cone. The actuator for deployment is a linear pneumatic cylinder.

The occulting mask wheel is purpose built for OSCA, as dictated by space and performance requirements. The wheel holds 10 masks that are glued into position. The mask wheel is rotated by an on-axis stepper motor and encoder, the encoder being used to confirm mask position. A pneumatically actuated pivoting detent arm locates in V-notches on the wheel circumference, providing a high level of accuracy and repeatability. Once the detent arm has locked the wheel in position the stepper motor is turned off; as the beam passes very close to the motor, having the motor turned off during observing ensures minimum contamination of the beam from heating effects. The co-alignment accuracy of masks is achieved by using the actual wheel unit and detent arm during assembly. After the first mask is glued in position an optical reference of its centre is made. The other masks are glued so that they are centred on this reference. This eliminates any errors due to machining inaccuracies.

The Lyot mask rotation is performed by a Newport SR50 step-motor rotator. This has an on-axis clear aperture that allows for easy mounting of the mask on to the rotator.

2.3 Performance simulations

Computer simulations have been performed for the coronagraph working with NAOMI. The simulations were used to determine optimum sizes of the key components (Lyot stop, focal masks) and to investigate the performance of the system. For the range of occulting mask sizes (0.25 – 2.0 arcsec) we found a suitable sized Lyot stop to be 80,20 (80% smaller primary and 20% oversized secondary masking). An additional Lyot stop was also manufactured of size 90,10. This provides adequate masking in the pupil plane when using focal plane masks of large 'effective diameter' (in units of λ/D) with the added benefit of increased system throughput. Figure 3 illustrates the change in light distribution in the pupil plane with 'effective diameter' of focal mask.

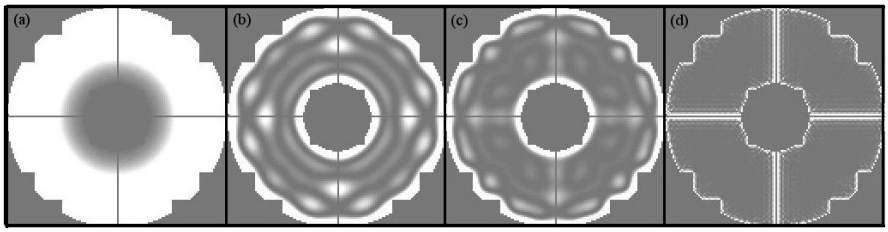

Figure 3. Simulated images of the OSCA pupil plane (flat wavefront). (a) λ = 2.2 μm, mask = 0.2 arcsec; (b) λ = 0.4 μm, mask = 0.2 arcsec; (c) λ = 2.2 μm, mask = 2.0 arcsec; (d) λ = 0.4 μm, mask = 2.0 arcsec

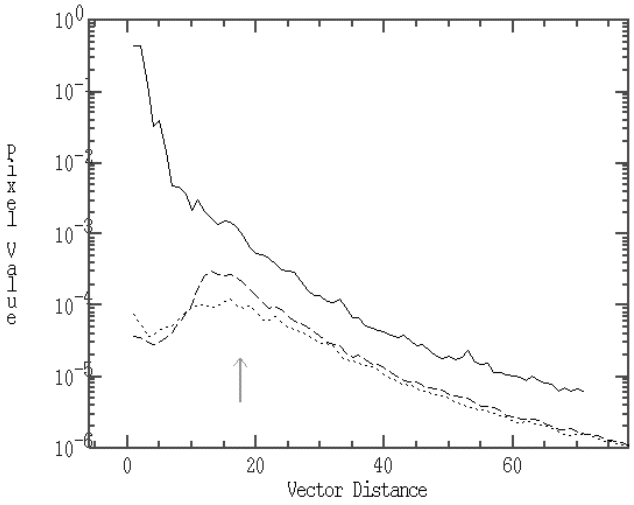

Figure 4. Computer simulation with (dashed line) and without (solid line) OSCA. Dotted line is for a gaussian shaped mask. Simulation represents performance of 2 arcsec mask at λ = 1.6 microns and seeing of 0.5 arcsec at 500nm.

As demonstrated in other papers [5] and in our own simulations an occulting mask consisting of a gaussian profile (opaque in the centre) achieves better suppression of the PSF in the final image compared to the traditional sharp edged disk. The simulation results in Figure 4 show a suppression factor of 4.3 at 0.5 arcsec from edge of mask (shown by arrow in figure). An improved suppression factor of 10 is gained by using a gaussian mask with a FWHM = diameter of solid disk.

3. COMMISSIONING

OSCA underwent its first commissioning run at the WHT between 19 and 25 May 2002. Two full nights (23 and 24) were taken for on-sky testing which were unfortunately plagued by bad seeing conditions. Only on the last night did the seeing improve to a level that was feasible to use the AO system.

3.1 Testing

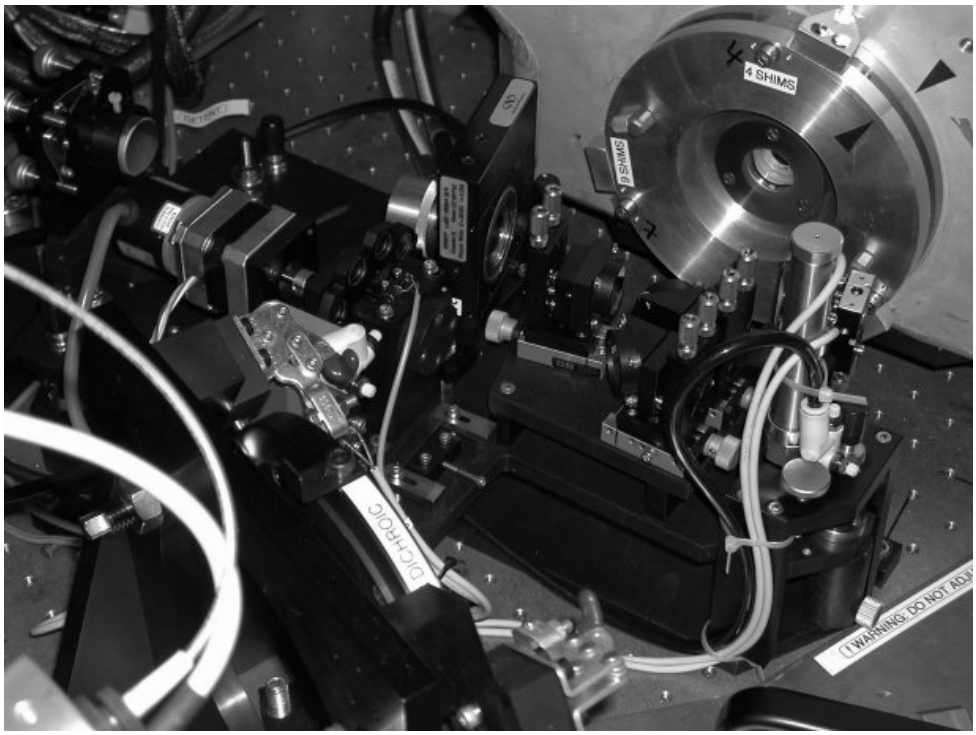

Figure 5. OSCA in place on the GHRIL bench at the WHT

OSCA was tested for its mechanism repeatability, accuracy of alignment and optical throughput. OSCA was deployed in and out of the beam several times and the position of a mask measured. On each instance the mask relocated to the same pixel position. Each occulting mask was selected in turn and the position of the centre measured. Taking the smallest mask as the reference the maximum displacement of a mask in pixels was (1,1) for the second to largest mask. This is well within the acceptable decentering criteria of about 10% mask diameter[1]. Since OSCA is located on the Nasmyth focus of the WHT, the pupil plane mask (Lyot stop) needs to rotate at the same rate as the field derotator to maintain the secondary vane masking. The rate of rotation of the Lyot stop was tested to be correct by viewing stars at several different sky elevations for some time and using INGRID in pupil viewing mode to check alignment between the Lyot stop and the secondary vanes. The centricity of rotation was within acceptable error margins. Optical throughput tests were performed in J and H and were found to be around 90%, as expected (correcting for Lyot stop masking).

3.2 On-sky performance

The night of 23 May was plagued by extremely bad seeing throughout (5 arcsec recorded at worst) and the AO system could not be used. Since the largest occulting mask in OSCA is 2 arcsec it was also not feasible to do any performance testing.

The last night saw an improvement in seeing (1.5 arcsec on average) which allowed us to use the AO system to give an average corrected PSF of 0.5 arcsec. Measurements of the suppression were obtained in J, H and Ks for some of the masks and are shown in Table 1.

Mask size (arcsec)	Corrected seeing (arcsec)	Wavelength band	Suppression (without/with)
2.00	0.40	J	2.0
2.00	0.45	Hcont	2.0
0.80	0.60	H	1.5
0.65	0.60	Ks	1.6

Table 1. Radially averaged suppression factors

Pixel counts were measured using a radial averaging program with values taken at approximately 0.5 arcsec from the edge of occulting mask. It should be noted that in directions away from the bright diffraction spikes (from the NAOMI square segments) the suppression factor is better than the averages recorded in Table 1. Figure 7 shows a cross section taken in such a favourable direction. In these directions OSCA obtains a suppression factor of approximately 3.2 (corrected for OSCA optical throughput). All masks need to be tested in good, steady seeing conditions to produce a fair performance comparison.

Attempts were made to observe some science targets during the course of the night. However due to limited time and poor seeing conditions the run was not successful in this respect.

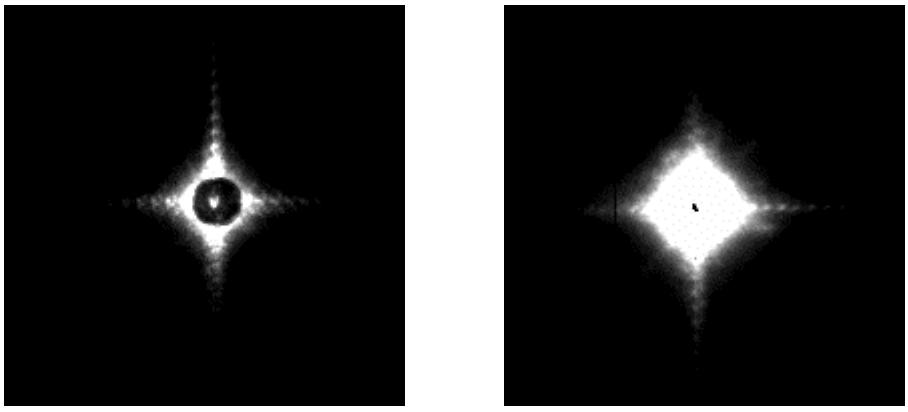

Figure 6. Dark subtracted image in Hcont band. Left is taken with OSCA (2” mask) and right is same object without OSCA. Both images are scaled to same level and were imaged through equivalent pupil plane masks.

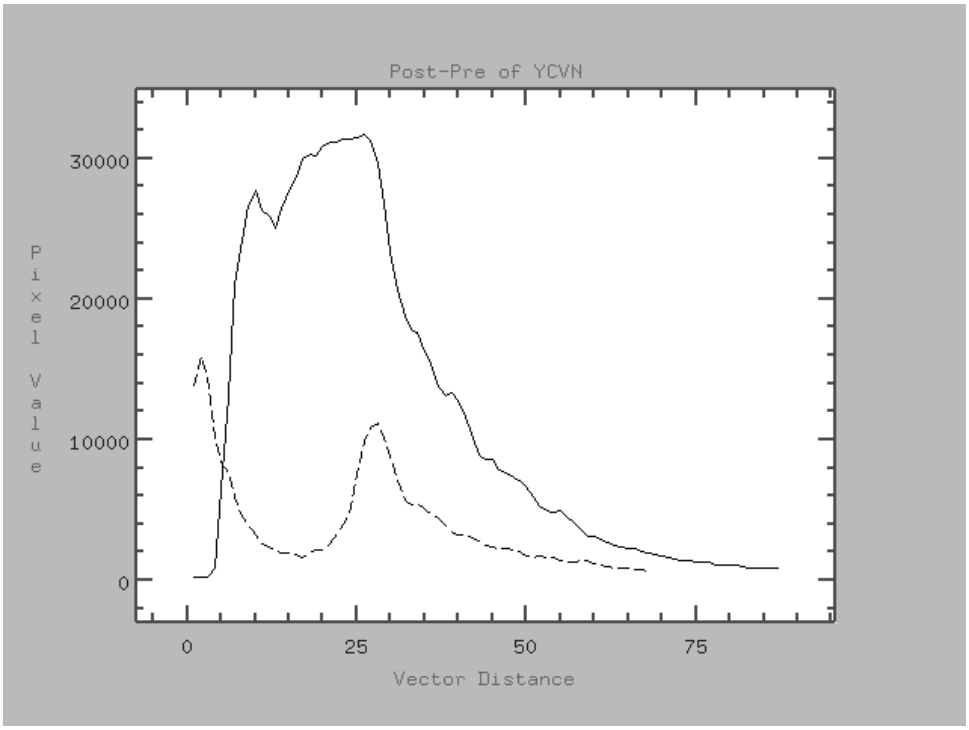

Figure 7. Cross-section through the images in Figure 6. The solid line is with no coronagraph and the dashed line is with OSCA in place. The peak at zero is due to the OSCA masks having a small throughput. The sharp drop at zero with no coronagraph is due to detector saturation. Vector distance is in pixels, the INGRID pixel scale is 0.04 arcsec/pixel.

3.3 Further work

More testing of OSCA is required in good seeing conditions to judge the best performance of the system and to allow the smaller masks to be tested. In these conditions observations of scientific interest can be undertaken. When a visible light camera is available (with OASIS commissioning) the gaussian masks on OSCA will be tested.

Some enhancements to OSCA may be added to reduce scattered light in the system. These include a razor edged baffle for each of the mask substrates and a pre-NAOMI dichroic stop. Simulations have shown this latter enhancement to further improve the suppression of OSCA. Since NAOMI uses visible light for wavefront sensing the dichroic stop would only let this wavelength through, thus reducing light scattered by the AO system at the science wavelength. However since this stop is before the AO system its size must be matched to the seeing disk. As the seeing can be so variable, a size of 1 arcsec is likely to be chosen and so this facility could only be used with the larger occulting masks.

ACKNOWLEDGMENTS

We would like to thank the Isaac Newton Group at the William Herschel Telescope for their support during the commissioning of OSCA. We also thank the astronomers at University College London and elsewhere that gave us help and suggestions for observing and objects of scientific interest. The funding for OSCA was provided by the UK Particle Physics and Astronomy Research Counsil (PPARC). SJT is grateful to UCL Graduate School and Physics department for funds to attend this conference. SJT also acknowledges PPARC for providing Ph.D. studentship.

REFERENCES

1. F. Malbet, “High angular resolution coronography for adaptive optics”, *A&ASS*, 115, pp. 161, 1996
2. R. B. Makidon, A. Sivaramakrishnan, C. D. Koresko, T. Berkefeld, M. J. Kuchner, and R. Winsor, “Ground-Based Coronagraphy with High Order Adaptive Optics, in *Adapive Optical Systems Technology*, P. L. Wizinowich, ed., *Proc SPIE* 4007, 2000
3. C. R. Benn, “Adaptive optics at the WHT”, *New Astronomy Reviews*, 45, pp. 59-62, 2001
4. M. B. Lyot, “A study of the solar corona and prominences without eclipse”, *MNRAS*, 99, pp. 580-594, 1939
5. T. Nakajima, “Planet detectability by an adaptive optics stellar coronagraph”, *ApJ*, 425, pp. 348-357, 1994